



ACCEPTED MANUSCRIPT

GaN Schottky diodes for proton beam monitoring

To cite this article before publication: Jean-Yves Duboz *et al* 2018 *Biomed. Phys. Eng. Express* in press <https://doi.org/10.1088/2057-1976/aaf9b4>

Manuscript version: Accepted Manuscript

Accepted Manuscript is “the version of the article accepted for publication including all changes made as a result of the peer review process, and which may also include the addition to the article by IOP Publishing of a header, an article ID, a cover sheet and/or an ‘Accepted Manuscript’ watermark, but excluding any other editing, typesetting or other changes made by IOP Publishing and/or its licensors”

This Accepted Manuscript is © 2018 IOP Publishing Ltd.

During the embargo period (the 12 month period from the publication of the Version of Record of this article), the Accepted Manuscript is fully protected by copyright and cannot be reused or reposted elsewhere.

As the Version of Record of this article is going to be / has been published on a subscription basis, this Accepted Manuscript is available for reuse under a CC BY-NC-ND 3.0 licence after the 12 month embargo period.

After the embargo period, everyone is permitted to use copy and redistribute this article for non-commercial purposes only, provided that they adhere to all the terms of the licence <https://creativecommons.org/licenses/by-nc-nd/3.0>

Although reasonable endeavours have been taken to obtain all necessary permissions from third parties to include their copyrighted content within this article, their full citation and copyright line may not be present in this Accepted Manuscript version. Before using any content from this article, please refer to the Version of Record on IOPscience once published for full citation and copyright details, as permissions will likely be required. All third party content is fully copyright protected, unless specifically stated otherwise in the figure caption in the Version of Record.

View the [article online](#) for updates and enhancements.

1
2
3 **GaN Schottky diodes for proton beam monitoring**
4
5
6
78 Jean-Yves Duboz^{*1}, Julie Zucchi¹, Eric Frayssinet¹, Patrick Chalbet¹, Sébastien Chenot¹,
910 Maxime Hugues¹, Jean-Claude Grini², Richard Trimaud², Marie Vidal² and Joël Héault²
1112 *1 Université Côte d'Azur, CNRS, CRHEA, 06560, Valbonne, France*
1314 *2-Université Côte d'Azur, Fédération Claude Lalanne;*
1516 *Cyclotron Biomédical, Centre Antoine Lacassagne, Nice, France*
1718 *Email : jyd@crhea.cnrs.fr*
1920
21
22
23
24
25
26
27
28
29
30
31
32
33 **Abstract**
34
35
36
37
38
39
40
41
42
43
44
45
46
47
48
49
50
51
52
53
54
55
56
57
58
59
60

We have demonstrated that GaN Schottky diodes can be used for high energy (64.8 MeV) proton beam monitoring. Such proton beams are used for tumor treatment, for which accurate and radiation resistant detectors are needed. GaN Schottky diodes have been measured to be highly sensitive to protons, to have a linear response with beam intensity and fast enough for the application. Some photoconductive gain was found in the diode leading to a good compromise between responsivity and response time. The imaging capability of GaN diodes in proton detection is also demonstrated.

1
2
3 AlGaN alloys are nowadays widely used for LEDs for lighting and displays, for laser in the
4 Blu-ray technology, and start to emerge for electronic applications in the radio frequency and
5 power domains. GaN is a wide band gap material with a strong chemical and mechanical
6 stability. The displacement energy is as large as 45 eV for the Ga atom and 109 eV for the N
7 atom [1]. As a result, GaN is expected to be more robust than many other semiconductors
8 against degradation under ionizing radiations. As an example, GaN based High Electron
9 Mobility Transistors are expected to stand 10 times higher doses than their GaAs cousins, partly
10 due to the difference in displacement energies and partly due to the piezoelectric field in nitrides
11 [2]. Ion implantation in GaN shows degradation thresholds in the range from 10^{14} cm^{-2} for heavy
12 ions at an energy of 500 keV to 10^{16} cm^{-2} for light ions at 10 keV [3]. The GaN device resistance
13 against radiation has been studied experimentally. Apart a few studies on LEDs [4], most
14 studies were devoted to Schottky diodes and transistors with the motivation of using GaN
15 electronics for space applications. For neutron irradiation, a degradation threshold was found
16 [5-7] for doses in the range of 10^{15} cm^{-2} . For proton irradiation, the threshold dose was found
17 to be above 10^{13} cm^{-2} for energies of 3 MeV [8] and degradation was clearly observed for a
18 dose of $2 \times 10^{15} \text{ cm}^{-2}$ for energies of 5 MeV [9]. A more detailed analysis of structural defects
19 created by an irradiation by 23 MeV protons at doses of $6 \times 10^{14} \text{ cm}^{-2}$ was reported [10, 11]. As
20 another benefit of its resistance to irradiation, GaN can be used for fabricating radiation hard
21 particle detectors [12] in harsh environments such as synchrotrons [13] or for fabricating X-ray
22 detectors for medical applications [14-16]. In the medical area, high energy particles are
23 commonly used for cancer treatment. In particular, proton-therapy is used in cases where the
24 tumor to be irradiated is close to vital and sensitive organs. A typical example is the eye tumor.
25 The irradiation must be limited to the tumor in the eye while sparing whenever possible macula
26 and optic nerve. For that, one takes advantage of a specific property of protons, which present
27 a very steep stopping profile in matter (Bragg peak) [17]. The proton dose has to be very well
28
29
30
31
32
33
34
35
36
37
38
39
40
41
42
43
44
45
46
47
48
49
50
51
52
53
54
55
56
57
58
59
60

1
2
3 controlled, with an accuracy better than 3%, and detectors are thus needed both *in vivo* (to
4 measure the dose during the patient irradiation) and on the beam (to monitor the beam prior to
5 irradiation). Silicon detectors are used but present long term degradation. Wide band gap
6 semiconductors have been proposed. Diamond is a good candidate due to its robustness and *in*
7 *vivo* compatibility and has been proposed a long time ago [18]. More recently, high
8 performance diamond based detectors have been reported for relative dosimetry application in
9 clinical proton beams, both at low energy and high energy and for both stationary/scattered and
10 scanned pencil beams. Diamond Schottky diodes [19, 20] and diamond photoconductors [21]
11 have been successfully demonstrated. After a development phase by Tor Vergata university in
12 Rome [19], diamond Schottky diodes are currently commercialized by the PTW Company
13 (microDiamond 60019) for proton dosimetry (70-230 MeV). They are however limited to small
14 sizes, well suited to dosimetry but less suited to external beam monitoring. On the contrary,
15 GaN benefits from its large deployment for optics and electronics, and is available in large
16 diameters and low costs, which allows fabricating larger detectors for beam monitoring. Let us
17 add for the sake of completion that GaN has also been proposed for *in vivo* dose monitoring
18 [22, 23], based on proton-luminescence. In this paper, we demonstrate for the first time that
19 GaN Schottky diodes can be used for beam monitoring.
20
21

22 Compared to vertical photoconductors with ohmic contacts, Schottky diodes offer the
23 advantage of smaller dark currents and faster transients. Compared to horizontal Metal-
24 Semiconductor-Metal detectors, vertical Schottky diodes offer a better charge collection in a
25 larger volume, which is a key parameter for protons with a large absorption depth. Finally, pn
26 junction offer similar advantages to Schottky diodes, with possible trapping issues in the Mg
27 doped region. As a result, Schottky diodes were chosen for this study. They have been
28 fabricated on a GaN layer grown by metal organic vapour phase epitaxy. A 20 μm thick non-
29 intentionally doped GaN layer was grown on a conductive (n-type) GaN substrate (Lumilog).
30
31
32
33
34
35
36
37
38
39
40
41
42
43
44
45
46
47
48
49
50
51
52
53
54
55
56
57
58
59
60

1
2
3 A TiAl ohmic contact was deposited on the back side first, and annealed at 750°C for 4 min.
4
5 Then large Schottky contacts were deposited on the front side, with an area varying between 1
6 and 2 mm², and based on 10 nm of Pt followed by 100 nm of Au. A SiO₂ passivation layer was
7 deposited next by Plasma Enhanced Chemical Vapor Deposition at 340°C. This deposition
8 lasted 2 hours and also acted as an annealing step for the Schottky contact. A thick metal layer
9 was finally deposited on the contact for facilitating the wire bonding. The final device is shown
10 in Fig.1. Samples with many diodes were mounted on ceramic chips with electrical connections.
11
12 All measurements were made at room temperature. Electrical measurements were performed
13 with a Keithley 2410-C Sourcemeter connected to the distant device through a 30 m coaxial
14 cable.
15

16
17
18
19
20
21
22
23
24
25
26
27
28
29
30
31
32
33
34
35
36
37
38
39
40
41
42
43
44
45
46
47
48
49
50
51
52
53
54
55
56
57
58
59
60
Diodes were tested first outside the proton beam. We refer these measurements as “in the dark”,
although it was in the light of the room (we checked that the diode were insensitive to the light
of the room). The diodes showed a rectifying behaviour, although not very strong, with some
dispersion on the dark current (I_d) among diodes, between 0.2 and 10 nA at -2V. Then the diodes
were measured in the proton beam of the MEDYCIC equipment, in the Lacassagne Proton-
therapy Center [24]. The isochrone cyclotron delivers proton pulses with a duration of 7 ns and
a frequency of 25 MHz. The beam is mono-energetic with a proton energy of 64.8 MeV. In the
present study, the device was in the air along the beam without any medium in front of it, so
that the incident proton energy is 64.8 MeV, which differs from the more complex set up used
for in vivo type measurements. The beam size on the detector position (upstream from the clinic
treatment room) is about 1 × 2 cm². Protons are incident on the front side of the sample.
Although the proton beam is pulsed, all measurements are performed in CW as pulses are not
resolved in our set up. The proton current can be varied from 10 pA to 100 nA. The total detector
current in the beam (I_t) was measured for various proton currents and diode biases. It was found
to be reproducible from diode to diode, within a factor of 2, and to be much larger than the dark

1
2
3 current. The response to the proton (called protocurrent I_p , not to be confused with the proton
4 current) is defined as the total current under the beam minus the dark current, $I_t - I_d$. Figure 2
5 shows, in log scale, the dark current and the protocurrent for one representative diode under a
6 proton beam current of 20 nA. We first observe that the protocurrent follows the same bias
7 dependence as the dark current. Second, at zero bias, the protocurrent is positive (0.47 μ A). It
8 changes sign between 0 and -0.1 V and then is negative for negative biases below -0.1V. Both
9 observations indicate that the diode is not working in the normal photovoltaic mode. Indeed,
10 the signal at zero bias should be negative, if it would originate from the Schottky depletion
11 region only. This result can be explained as follows. The penetration depth of 64.8 MeV proton
12 in GaN is a few mm, while the depletion region below the Schottky contact is few μ m thick,
13 the un-doped region is 20 μ m thick and the substrate is 350 μ m thick. Hence most of the
14 absorption is in the doped substrate, where carriers rapidly recombine, as the field remains small
15 even under an applied bias. We assume that the substrate contribution remains negligible except
16 close to zero volt. A very small absorption occurs in the depletion region, leading to a small
17 negative signal, and which should increase as the depletion region width, i.e. as $(\Phi - e \times V)^{1/2}$,
18 where Φ is the Schottky barrier height, e is the electron charge and V is the applied bias. An
19 intermediately large absorption occurs in the un-doped layer, where the field is close to zero at
20 zero bias, but becomes non negligible under bias. This leads to a contribution which changes
21 sign with bias. Secondary electron emission from the Schottky metal contact may also
22 contribute and lead to a positive signal at zero bias. Finally, a photovoltaic effect on the back
23 side of the sample could also be considered, leading to a positive signal at zero bias. The signal
24 at zero bias results from all contributions, and turns out to be positive. Under an applied voltage,
25 the contribution of the un-doped region dominates and leads to a photoconductive behaviour.
26 Photoconductive behaviour results from the capture of either the electron or the hole while the
27 other carrier is collected [25]. In GaN, the hole is generally trapped [26]. In order to maintain
28
29
30
31
32
33
34
35
36
37
38
39
40
41
42
43
44
45
46
47
48
49
50
51
52
53
54
55
56
57
58
59
60

1
2
3 the electrical neutrality, the device injects electrons until one electron recombines with the
4 trapped hole. This electron injection leads to the photoconductive gain [25]. This process may
5 happen in the bulk [26, 27] or close to the surface [28]. In other words, the Schottky diode can
6 be modelled as a rectifying contact in series with a resistance (un-doped region). Due to
7 processing problems, the Schottky contact is not strongly rectifying and the current is mostly
8 limited by the resistive layer, both in the dark and under the proton beam. This leads to a
9 photoconductive behaviour. Please note that the same diode may have a photovoltaic behaviour
10 under UV illumination as the absorption would be in the depletion layer only. Hence, the
11 observed photoconductive behaviour in the proton beam is largely due to the large penetration
12 depth of protons. When turning the beam on, we observed that the protocurrent was rapidly
13 increasing to 90% of its final value, and then increasing within a few seconds to its final value.
14 This slow transient is typical for a photoconductive behaviour. A similar behaviour was
15 observed during turn-off. Note that the fast transient could not be observed with a resolution
16 better than a fraction of second, so that it may also reveal a photoconductive behavior, although
17 with a faster component than the observed slow transient.

18
19
20
21
22
23
24
25
26
27
28
29
30
31
32
33
34
35
36
37
38
39
40
41
42
43
44
45
46
47
48
49
50
51
52
53
54
55
56
57
58
59
60 We will now discuss the absolute value of the protocurrent. Poly-methyl methacrylate (PMMA) is often used for proton dose calibration as its density is not too far the one of living tissues. The absorption depth in PMMA has been measured to be 29 mm. The density of GaN is 6.15 g/cm³ while the PMMA one is 1.18g/cm³, so that the absorption is stronger in GaN than in PMMA. The absorption depth calculated in GaN is supposed to be 8.6mm according to SRIM 2013 data tables [29]. This absorption depth is much larger than the device active region, we are in the plateau region of the energy deposition profile. Hence we can take a uniform absorption in depth so that the absorption in a GaN layer of thickness W (in μm) is $W/8600$. The power deposited by the beam of section S in the diode of section s is $W/8600 \times E \times I_p \times s/S$, where E is the proton energy and I_p the proton current. We then assume that protons obey the

1
2
3 following rule of thumb: the energy needed to create an electron hole pair is three times the gap
4 energy, i.e. about 10 eV. The charge created per second in the diode is then
5 $W/8600 \times E \times I_p \times s / (3 \times E_g)$. In a photovoltaic mode, without gain and with a unity collection
6 efficiency, this charge created per second is equal to the protocurrent. Under a reverse bias of -
7 2V, the depletion region W can be estimated to be about 4 μm . With $s=1 \text{ mm}^2$ and $S=2 \text{ cm}^2$, the
8 calculation leads to a protocurrent of about $0.2\mu\text{A}$. We have experimentally measured $100\mu\text{A}$,
9 which clearly shows that there is such photoconductive gain in the diode, confirming our
10 assertion of a photoconductive behavior.
11
12

13 The diode response has been measured as a function of the proton beam current, from 10 pA
14 up to 100 nA. Figure 3 shows the result (I_p) for various diode biases. We observe an excellent
15 linearity over 5 decades.
16
17

18 One difficulty in the measurements was that the sample and sample holder became
19 radioactive (^{15}O , ^{14}O , ^{68}Ge , ^{69}Ge , ^{71}Ge are the most likely produced isotopes) after exposure to
20 the proton beam, and then impossible to handle. Hence, we tried to minimize the exposure time.
21 In total, we can estimate that each sample remained at least 15 min in the beam, with an average
22 current of 20 nA. This gives a cumulated dose larger than $0.5 \times 10^{14} \text{ cm}^{-2}$. We sometimes
23 observed that the dark current in reverse bias increased after a beam exposure, in particular
24 when it was originally very small, but returned to its initial value after some time (less than one
25 hour) or after application of a positive bias. Hence, the dark current change was mostly due to
26 the proto-generation of charges and their subsequent trapping. No real degradation could be
27 observed from electrical characteristics, which is a first indication of the GaN resistance to
28 ionizing radiations. Longer-time tests remain however needed to have a qualitative idea of the
29 radiation hardness and possible effects of radiation damage on device performance.
30
31

32 We have used the Schottky diodes to monitor the proton beam shape. The sample was
33 mounted on a translation stage positioned in the center of the beam in the vertical direction
34
35
36
37
38
39
40
41
42
43
44
45
46
47
48
49
50
51
52
53
54
55
56
57
58
59
60

(beam size about 2 cm in the vertical direction), and was moved in the horizontal direction over 5 cm (beam size on the order of 1 cm) across the beam. The signal was recorded as a function of position, thus giving the beam shape. Two diodes separated by about 3 mm on the same sample have been used. Figure 4 shows the result recorded at -2V. The scan duration is about 1 min, which is much larger than the device response time. Hence, the device response time does not alter the profile, as demonstrated by the acquisition of the same profiles in both translation directions. The beam profile is slightly asymmetric, with a full width at half maximum of about 7.6 mm. The measured profile is the convolution of the actual beam profile and the detector width (1mm). The beam profile can be deduced from Fig.4 and is actually found to be close to 7.6mm. As an approximation, the convolution of two Gaussian profiles of width W_1 and W_2 gives a Gaussian profile with a width $W = \sqrt{W_1^2 + W_2^2}$. Hence, the beam profile is given by $\sqrt{7.6^2 - 1^2} = 7.53\text{mm}$. A similar profile was obtained at 0V but with a slightly larger width of 8.2mm. This shows that the beam profile is convoluted with a larger detector width of approximately 3mm: This may indicate that at 0V, the signal is mainly arising from the back side of the sample, which is about 3 to 4 mm wide. Finally, the beam profile was measured with a Si diode (pin BP 104F) mounted so as to detect protons from the edge of the diode, corresponding to an effective width equal to the depletion zone, id est less than 10 μm . The full width at half maximum was found to be about 7.5mm (Fig.4), with a clear asymmetry, which confirms the measurements based on GaN Schottky diodes. The peak positions measured by the two GaN diodes differ by about 3 mm, as expected from their separation on the sample. This shows that these Schottky diodes, if they are fabricated in an array, can be used for proton imaging. Typical sizes and periods for such an array of Schottky diodes would be about 100 μm for the proton-therapy application, and are easy to obtain from the technological point of view.

1
2
3 In conclusion, we have demonstrated that GaN Schottky diodes can be used to monitor
4 proton beams at 64.8 MeV used for proton-therapy. Protons could be detected down to the
5 smallest possible current, hence the sensitivity is high enough for the application. Diodes are
6 linear in power, which is of prime importance for an accurate monitoring. They are resistant to
7 degradation up to a dose of at least $0.5 \times 10^{14} \text{ cm}^{-2}$. Time response is short enough (s) for the
8 envisaged application. Some issues remain on elucidating the exact contribution of various parts
9 of the device. Improvements in the processing and some changes in the epitaxial structure are
10 likely to improve the device performance up to a commercial level. Best application of such
11 devices fabricated in arrays is likely to be external beam monitoring.
12
13
14
15
16
17
18
19
20
21
22
23
24
25
26
27
28
29
30
31
32
33
34
35
36
37
38
39
40
41
42
43
44
45
46
47
48
49
50
51
52
53
54
55
56
57
58
59
60

Acknowledgements

We acknowledge support from GANEX (ANR-11-LABX-0014). GANEX belongs to the
public funded 'Investissements d'Avenir' program managed by the French ANR agency.

1
2
3
4
5
REFERENCES

6 [1] S. J. Pearton and R. Deist, Review of radiation damage in GaN-based materials and devices,
7 Journal of Vacuum Science & Technology A31, 050801 (2013).

8 [2] B. D. Weaver, T.J. Anderson, A.D. Koehler, J.D. Greenlee, J.K. Hite, D.I. Shahin, F.J. Kub,
9 and K.D. Hobart, On the Radiation Tolerance of AlGaN/GaN HEMTs Electronic and Photonic
10 Devices and Systems, ECS Journal of Solid State Science and Technology 5, (7) Q208-Q212
11 (2016).

12 [3] S. O. Kucheyev, J. S. Williams, C. Jagadish, J. Zou, G. Li, and A. I. Titov, Effect of ion
13 species on the accumulation of ion-beam damage in GaN, Phys. Rev. B 64, 035202 (2001).

14 [4] A. Floriduz and J. D. Devine, Modelling of proton irradiated GaN-based high power white
15 light-emitting diodes, *Jpn. J. Appl. Phys.* **57**, 080304 (2018).

16 [5] P. Mulligan, J. Qiu; J. Wang ; L. R. Cao, Study of GaN radiation sensor after in-core neutron
17 irradiation, IEEE Transactions on Nuclear Science, 61, 1-5 (2013).

18 [6] E Gaubas, T Ceponis, L Deveikis, D Meskauskaitė, S Miasojedovas, J Mickevicius, J
19 Pavlov, K Pukas, J Vaitkus, M Velicka, M Zajac and R Kucharski, Study of neutron irradiated
20 structures of ammonothermal GaN, Journal of Physics D: Applied Physics, 50, 13, 135102
21 (2017).

22 [7] J. Wang, P. Mulligan, L. Brillson, and L. R. Cao, Review of using gallium nitride for
23 ionizing radiation detection, *Applied Physics Reviews* **2**, 031102 (2015).

24 [8] A. Stocco, S.Gerardin, D.Bisi, S.Dalcanale, F.Rampazzo, M.Meneghini, G.Meneghesso,
25 J.Grünenpütt, B.Lambert, H.Blanck, E.Zanoni, Proton induced trapping effect on space
26 compatible GaN HEMTs, *Microelectronics Reliability* **54**, 2213–2216 (2014).

27 [9] H.-Y. Kim, T. Anderson, M.A. Mastro, J. A. Freitas Jr, S. Jang, J. Hite, C. R. Eddy Jr, J.
28 Kim, Optical and electrical characterization of AlGaN/GaN high electron mobility transistors
29 irradiated with 5MeV protons, *Journal of Crystal Growth* **326**, 1, 62-64 (2011).

[10] T.J. Anderson, A. D. Koehler, J. D. Greenlee, B. D. Weaver, M. A. Mastro, J. K. Hite, C. R. Eddy, F. J. Kub, and K. D. Hobart., Substrate-Dependent Effects on the Response of AlGaN/GaN HEMTs to 2-MeV Proton Irradiation, *IEEE Electron Dev. Lett.* **35** (8), 826-828 (2014).

[11] A. D. Koehler, P. Specht, T. J. Anderson, B. D. Weaver, J. D. Greenlee, M. J. Tadjer, M. Porter, M. Wade, O. C. Dubon, K. D. Hobart, T. R. Weatherford, and F. J. Kub, Proton Radiation-Induced Void Formation in Ni/Au-Gated AlGaN/GaN HEMTs, *IEEE Electron Device Letters* **35**, 12, 1194 – 1196 (2014).

[12] Proceedings of the 6th International Workshop on Radiation Imaging Detectors, Glasgow 2004, Nuclear Instruments and Methods in Physics Research Section A: Accelerators, Spectrometers, Detectors and Associated Equipment. **546**, (1-2), 1-344 (2005).

[13] J. Grant, R. Bates, W. Cunningham, A. Blue, J. Melone, F. McEwan, J. Vaitkus, E. Gaubas, V. O’Shea, GaN as a radiation hard particle detector, *Nuclear Instruments and Methods in Physics Research Section A: Accelerators, Spectrometers, Detectors and Associated Equipment*, **576**, 1, 60-65, (2007).

[14] J.Y. Duboz, M. Laügt, D. Schenk, B. Beaumont, J.L. Reverchon, A. Wieck, and T. Zimmerling, “GaN for x-ray detection”, *Appl. Phys. Lett.* **92**, 263501 (2008).

[15] J.-Y. Duboz, B. Beaumont, J.-L. Reverchon, and A. D. Wieck, “Anomalous photoresponse of GaN X-ray Schottky detectors”, *J. Appl. Phys.* **105**, 114512 (2009).

[16] J.-Y. Duboz, E. Frayssinet, S. Chenot, J.-L. Reverchon, and M. Idir, “X-ray detectors based on GaN Schottky diodes”, *Appl. Phys. Lett.* **97**, 163507 (2010).

[17] H.Paganetti and T. Bortfeld, Proton Beam Radiotherapy - The State of the Art, New Technologies in Radiation Oncology (Medical Radiology Series), Eds. W. Schlegel, T. Bortfeld and A.-L. Grosu, Springer Verlag, Heidelberg, ISBN 3-540-00321-5, (2005).

[18] T. L. Nam, R. J. Keddy, and R. C. Burns, Synthetic diamonds as *in vivo* radiation detectors, *Medical physics* 14, 4, 596-601 (1987).

[19] M. Marinelli, F. Pompili, G. Prestopino, C. Verona, G. Verona-Rinati, G. A. P. Cirrone, G. Cuttone, R. M. La Rosa, L. Raffaele, F. Romano, C. Tuvè, Dosimetric characterization of a synthetic single crystal diamond detector in a clinical 62 MeV ocular therapy proton beam, *Nuclear Instruments and Methods in Physics Research A* 767, 310–317 (2014).

[20] S. Rossomme, J. M. Denis, K. Souris, A. Delor, F. Bartier, D. Dumont, S. Vynckier, and H. Palmans, LET dependence of the response of a PTW-60019 micro-Diamond detector in a 62 MeV proton beam, *Physica Medica* 32, 1135–1138 (2016).

[21] C. Moignier, D. Tromson, L. de Marzi, F. Marsolat, J. C. G. Hernández, M. Agelou, M. Pomorski, R. Woo, J.-M. Bourbotte, F. Moignau, D. Lazaro, and A. Mazal, Development of a synthetic single crystal diamond dosimeter for dose measurement of clinical proton beams, *Physics in Medicine and Biology* 62 (13), 5417-5439 (2017).

[22] A. Ismail, P. Pittet, G. N. Lu, J. M. Galvan, J. Y. Giraud, and J. Balosso In vivo dosimetric system based on Gallium Nitride radioluminescence, *Radiation Measurements* 46, 1960-1962 (2011).

[23] P. Pittet, A. Ismail, J. Ribouton, R. Wang, J.-M. Galvan, A. Chaikh, G.-N. Lu, P. Jalade, J.-Y. Giraud, and J. Balosso. Fiber background rejection and crystal over-response compensation for GaN based in vivo dosimetry, *Physica Medica*, 29, 5, 487 (2013).

[24] <http://www.centreantoinelacassagne.org/qui-sommes-nous/les-poles/pole-de-radiotherapie/>

[25] S.M. Sze, *Physics of semiconductors*, Wiley-Interscience, New Jersey, USA (2007).

[26] F. Binet, J.Y. Duboz, E. Rosencher, F. Scholz, and V. Härle, « Mechanisms of recombination in GaN photoconductors », *Appl. Phys. Lett.* 69, 1202 (1996).

1
2
3 [27] J. A. Garrido, E. Monroy, I. Izpura and E. Muñoz, Photoconductive gain modelling of
4
5 GaN photodetectors, *Semiconductor Science and Technology*, 13 (6), 563 (1998).
6
7
8

9 [28] Schubert F. Soares, Photoconductive Gain in a Schottky Barrier Photodiode, *Japanese*
10
11 Journal of Applied Physics, Volume 31, Part 1, Number 2A (1992).
12
13

14 [29] J. F. Ziegler, The Stopping and Range of Ions in Matter, <http://www.srim.org>
15
16
17
18
19
20
21
22
23
24
25
26
27
28
29
30
31
32
33
34
35
36
37
38
39
40
41
42
43
44
45
46
47
48
49
50
51
52
53
54
55
56
57
58
59
60

1
2
3 FIGURE CAPTIONS
4
5
6
7
8
910 FIGURE 1: Schematic of the GaN Schottky diode and the electrical circuit.
11
1213 FIGURE 2: Current versus voltage for a Schottky diode in the dark (black square) and under
14 proton irradiation (proton beam current is 20 nA) (red triangle).
15
1617 FIGURE 3: Protocurrent in the Schottky diode under proton irradiation versus proton beam
18 intensity, for various detector biases
19
2021 FIGURE 4: Normalized protocurrent in two Schottky diodes, and in a Si diode as a function of
22 the translation stage position. The currents at a bias of -2V were -5.3 and -7.3 μ A for diodes A
23 and B respectively. Proton current is 10 nA.
24
25
26
27
28
29
30
31
32
33
34
35
36
37
38
39
40
41
42
43
44
45
46
47
48
49
50
51
52
53
54
55
56
57
58
59
60

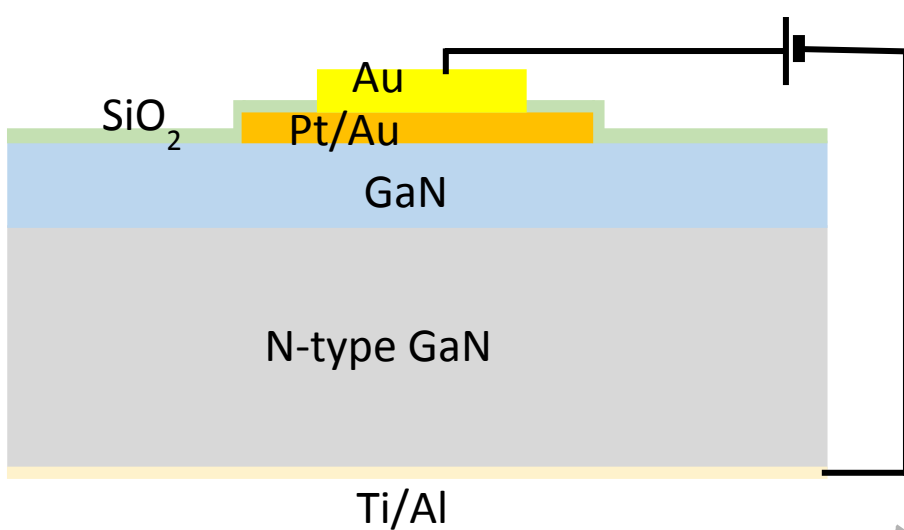


FIGURE 1

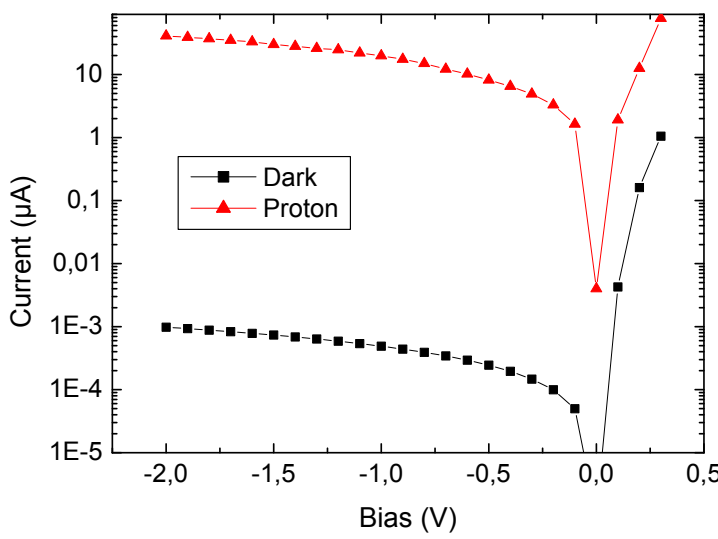


FIGURE 2

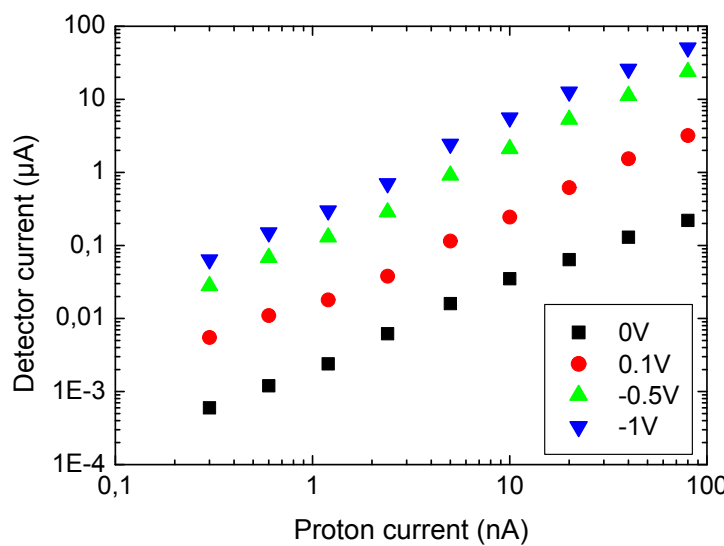


FIGURE 3

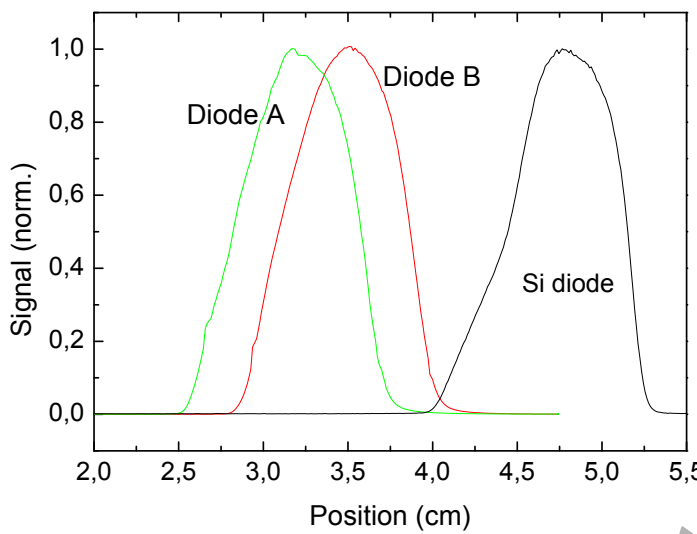


FIGURE 4